Journal of Materials Chemistry A

Accepted Manuscript

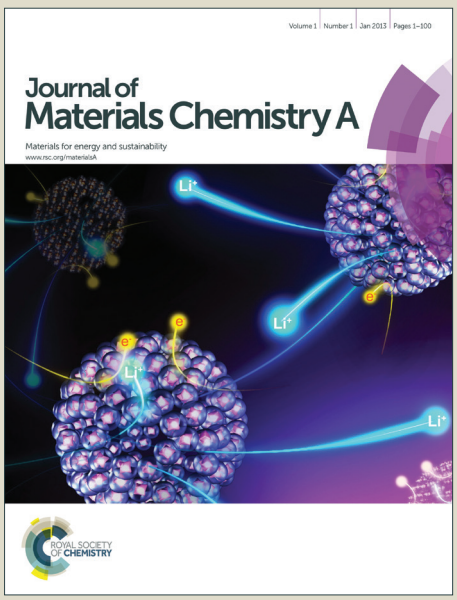

ROYAL SOCIETY OF CHEMISTRY

www.rsc.org/materialsA

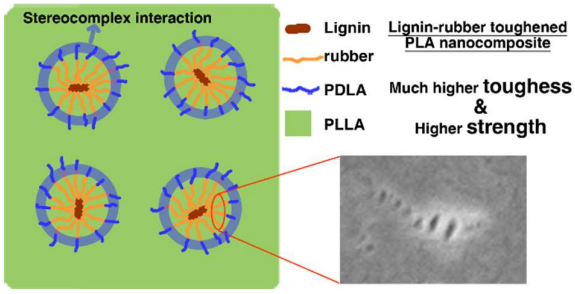

TOC/Abstract graphic

SYNOPSIS

Lignin, a biomass, is grafted with biodegradable rubber to simultaneously toughen and strengthen poly (lactide), owing to strong matrix-filler interaction and existence of rubber between "rigid" lignin and matrix facilitating force transfer and craze formation.

Journal of Materials Chemistry A

RSCPublishing

ARTICLE

Biodegradable and Renewable Poly (lactide)-Lignin Composites: Synthesis, Interface and Toughening Mechanism

Cite this: DOI: 10.1039/xoxxoooooox

Received ooth January 2012,
Accepted ooth January 2012

DOI: 10.1039/xoxxoooooox

www.rsc.org/

Yang Sun,[a] Liping Yang,[b] Xuehong Lu[c] and Chaobin He[a,d,*]

Poly (lactide) (PLA)-lignin composites were fabricated by blending lignin-*g*-rubber-*g*-poly (D-lactide) copolymer particles and commercial poly (L-lactide) (PLLA) in chloroform. To synthesize the copolymer, poly (ε-caprolactone-*co*-lactide) (PCLLA) rubbery layer was formed *via* lignin-initiated ring opening copolymerization of ε-caprolactone/L-lactide mixture, followed by the formation of poly (D-lactide) (PDLA) outer segments *via* polymerization of D-lactide. The PDLA segments may contribute to strong interfacial interactions between lignin-rubber-PDLA and PLLA matrix by stereocomplexation which was observed using differential scanning calorimetry (DSC), Fourier transform infrared spectroscopy (FT-IR) and wide angle X-ray scattering (WAXS). The quasi-random structure of PCLLA and the formation of outer PDLA segments were characterized by nuclear magnetic resonance (NMR). A T_g of ~-36 °C for PCLLA was detected by DSC, which confirms the rubbery characteristic of the synthesized copolymer. The resulting renewable and biodegradable composites exhibited a six-fold increase of elongation at break and a simultaneous improvement of tensile strength and Young's modulus albeit to a lesser extent. Light scattering, WAXS, small angle X-ray scattering (SAXS) and scanning electron microscope (SEM) studies suggested that good lignin dispersion, rubber-initiated crazing and strong filler-matrix interactions due to stereocomplexation are the effective mechanisms behind the excellent mechanical performances.

Introduction

Lignin is an abundant renewable lignocellulosic biomass extracted from agricultural waste, such as forest thinnings, rice stalk, wheat straw, and cotton linters.[1] It is a randomly crosslinked network biopolymer based on phenylpropanoid monomer structure and can be found within cell walls and between cells, endowing the plant with both structural rigidity and resistance to biological attack.[2] *In vitro*, lignin has been shown to exhibit antimicrobial and antifungal activity,[3] antioxidation[4] and ultraviolet (UV) radiation absorption[5]. However, lignin is often disposed of as an industrial waste or by combustion to produce heat. In recent years, strong global interests arise in renewable energy and plant-derived chemical feedstocks due to limited reserves of fossil fuel resources.[1] Consequently, using lignin to develop value-added products becomes attractive in research areas of materials and chemistry, among which is the fabrication of polymer-lignin composites[6-10]. Unmodified lignin tends to aggregate in polymer composites due to π–π stacking of aromatic rings, and hydrogen bonding and van der Waals attraction among polymer chains[11, 12], which would impair the properties of the resulting composites. To overcome this, grafting polymerization of synthetic polymer chains on lignin offers an effective solution. For example, Tadamasa Nemoto, et al.[8] prepared lignin-graft poly(2-ethyl-2-oxazoline) that could produce novel lignin-based polymer blends with polystyrene, poly(vinyl chloride), and polyvinylpyrrolidone.

Poly (lactide) (PLA) is a polymer derived from plant sources with good biodegradability and biocompatibility,[13, 14] and it basically has three isomers: poly (D-lactide) (PDLA), poly (L-lactide) (PLLA), and poly (racemic-lactide) (PDLLA). Currently, PLA's bio-renewability and good mechanical

properties have made it promising to replace polymers derived from petroleum sources.[14] However, the massive commercial applications of PLA are hindered by its drawbacks such as small elongation at break (<10 %), poor impact strength (~5 kJ/m^2), low heat deflection temperature (<60 °C) and poor UV light barrier properties.[15] Lignin has been added into PLA to achieve renewable composites,[16-18] which however hardly exhibit desirable improvements in elongation at break thus still resulting in brittleness. On the other hand, rubber phase is frequently added to improve the toughness of PLA composites,[19-22] but always at the expense of modulus and tensile strength. In our previous work,[23] rigid polyhedral oligomeric silsesquioxane (POSS) was grafted with rubber to successfully toughen PLA with a ten-fold increase in ductility while maintain the high modulus of PLA. Hence, it is anticipated that by using lignin as a "rigid core", lignin-g-rubber-g-PDLA could also toughen PLA without impairing the high tensile strength and modulus of the matrix.

In this paper, fully biodegradable and renewable lignin-rubber-PDLA copolymer for toughening PLLA matrix was synthesized as shown in Scheme 1, in which two stages were involved: First, poly (caprolactone-*co*-lactide) (PCLLA) was grafted onto lignin *via* ring opening copolymerization of ε-caprolactone (ε-CL) and lactide monomers, initiated by the alkyl alcohol functional groups on lignin, to form the rubbery phase. Poly (ε-caprolactone) (PCL) is a biodegradable polymer with nontoxicity and permeability.[24] Various studies have been carried out on block and random copolymers of LA and ε-CL.[24-27] Particularly, PCLLA exhibits rubbery elasticity due to its physically cross-linked structure, and the monomer ratio can alter PCLLA's mechanical properties.[28] Besides, PCLLA is fully biodegradable. Second, poly (D-lactide) (PDLA) was subsequently polymerized onto the rubbery phase to serve as the compatibilizer. Stereocomplex crystallite (sc-crystallite) could be formed between PDLA and PLLA in solid state from the melt or in solution,[29] which exhibits different properties from PLLA or PDLA homocrystallite.[30] Stereocomplexation in PLA has been extensively studied,[14, 30-35] and it is found that high concentrations of non-conventional hydrogen bonds exist in the sc-crystallite,[36] which may account for the better mechanical properties and thermal resistance of sc-crystallites compared with PLA homocrystallites. Hence, stereocomplexation between PDLA compatibilizer and PLLA matrix can contribute to strong interactions at the interface of lignin-rubber copolymer and PLLA matrix and thus facilitate effective force transfer and better filler dispersion.

PLA nanocomposites, which were formed through blending the synthesized lignin-rubber-PDLA copolymer and commercial PLLA, exhibit a six-fold increase of elongation at break and simultaneous improvements of tensile strength and Young's modulus. Crazing, strong stereocomplex interaction, and good particle dispersion are the possible mechanisms behind the excellent mechanical performances. Furthermore, attributed to the UV absorption property of lignin, the renewable nanocomposites showed good UV light barrier characteristics compared with neat PLLA, which would be useful in packaging application. Our system is unique as the rubber phase is biodegradable and biocompatible while the toughening effect is significant without reducing modulus and tensile strength. On the other hand, our study demonstrates the importance of interfacial interaction in tailoring the mechanical property of polymer composites.

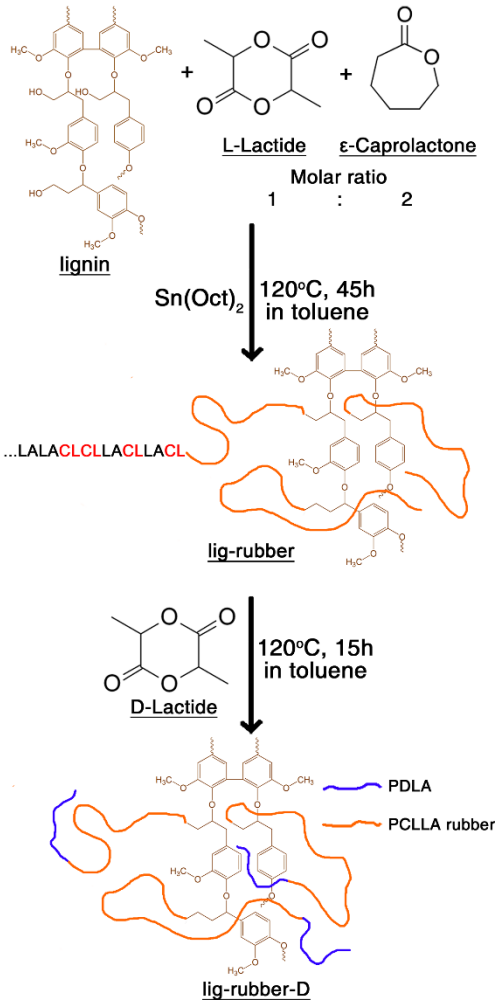

Scheme 1 Route to synthesize lig-rubber-D *via* ring opening polymerization.

Experimental

Materials

Lactide monomers (D- and L-, purity is 99.5 %) were purchased from Purac. Before polymerization, the monomers were recrystallized in ethyl acetate for 3 times. Lignin (organosolv) was purchased from Sigma Aldrich. ε-Caprolactone (ε-CL) was received from Sigma-Aldrich and dried by distillation under reduced pressure. PLLA (product number: 3051D, 96.5 % of L-lactide, M_w: 160000, PDI: 1.7) pellets were obtained from Natureworks. Anhydrous toluene and tin (II)2-ethylhexanoate ($Sn(Oct)_2$, 95 %) were received from Sigma-Aldrich and used as the solvent and catalyst respectively in the ring opening polymerization. Lactide and lignin were dried in vacuum oven for 12 h before use at 40 °C and 120 °C respectively. All the other chemicals were used as adopted.

Synthesis of lignin-rubber-PDLA, lignin-rubber-PLLA and lignin-PDLA

Lignin-rubber-PDLA, the renewable copolymer, was synthesized in two stages *via* ring opening polymerization (ROP) (Scheme 1). In the first stage, to synthesize lignin-rubber, ROP of L-lactide/ε-CL mixture in a molar ratio of 1:2 was carried out, initiated by the alkyl alcohol functional groups on

lignin. Specifically, lignin (0.2 g) and ε-CL (9.19 g, 80.6 mmol) were charged into a 150 ml round bottom flask, which was then stirred at 50 ℃ in Ar for half an hour to obtain a homogeneous mixture. $Sn(Oct)_2$ (160 μL), L-lactide (5.81 g, 40.3 mmol), and anhydrous toluene (100 ml) were subsequently charged. The chemical charging should be performed in glove box. The homogeneous mixture was refluxed and stirred at 120 ℃ in Ar. After 45 h, 2 ml of reaction mixture was withdrawn and precipitated in excess methanol. The obtained sticky lignin-poly (caprolactone-*co*-lactide) (PCLLA) rubber copolymer was then centrifuged and washed in methanol for 3 times, which is denoted as lig-rubber. In the second stage, D-lactide (5.00 g, 34.7 mmol) was further charged and the ROP continued for another 15 h. After the reaction, the lignin-rubber-PDLA copolymer was dissolved by chloroform, precipitated in excess methanol and filtered with methanol wash, which is denoted as lig-rubber-D. Lig-rubber and lig-rubber-D were dried in vacuum for 12 h at 40 ºC. The yield of lig-rubber-D was 89 wt%.

To study the effect of interfacial interaction such as stereocomplexation on the properties of final nanocomposites, lignin-g-rubber-g-PLLA, denoted as lig-rubber-L, was synthesized as the control. The synthesis route is the same as that of lig-rubber-D except that L-lactide replaced D-lactide in the second stage.

To investigate the effect of rubber phases at the interface of "rigid filler" lignin and PLA matrix on toughening, lignin-PDLA without rubber was synthesized *via* ROP of D-lactide as follows: 0.2 g lignin was added into a flask equipped with a magnetic stirring bar, and purged with Ar for 30mins, then D-lactide (4 g) and $Sn(OCt)_2$ (20 mg) were added into the system. Ar purging continued for another 30 mins, followed by heating to 150 ℃ and keeping for 4 hours. At the end of the reaction, lignin-PDLA, denoted as lig-D, was dissolved by chloroform, precipitated in excess methanol and filtered with methanol wash.

Fabrication of biodegradable and renewable nanocomposites

Chloroform solution of commercial PLLA was prepared first, and then lig-rubber-D was added. The final solution, with a concentration of around 100 mg/ml, was casted, at ambient conditions for 12 h and at 80 ºC in vacuum for another 12 h, to form nanocomposites of various compositions denoted as X%-lig-rubber-D, in which X represents lig-rubber-D content, i.e., 15 wt %, 10 wt % and 5 wt %. Commercial PLLA films were fabricated in a similar way without lig-rubber-D added. Control samples (2%-lig-D, 5%-lig-rubber-L, 10%-lig-rubber-L, 15%-lig-rubber-L) were also prepared likewise. The nanocomposite films, 0.5 mm in thickness, were stored at 25 ºC in a dry cabinet before characterizations.

Characterizations

Fourier transform infrared spectroscopy (FT-IR) tests were done on a PerkinElmer 2000 spectrometer at a resolution of 1 cm^{-1}. Nuclear magnetic resonance (NMR) spectra were obtained on a Bruker 400 MHz NMR spectrometer in $CDCl_3$ at room temperature. Normal and modulated differential scanning calorimetry (DSC) experiments were carried out on TA Instrument Q100 under N_2. To measure T_g of the synthesized polymers, modulated DSC (MDSC) was employed as follows: equilibrate at 25 ℃; ramp 20 ℃ /min to 230 ℃; isothermal for 5 min; ramp 20 ℃ /min to -80 ℃; isothermal for 2 min; modulate +/- 2.00 ℃ every 40 seconds; ramp 10 ℃ /min to 230 ℃. Wide-angle X-ray scattering (WAXS) tests were performed on a Bruker GADDS diffractometer (area detector) operating at 40 mA and 40 kV. Small-angle X-ray scattering tests were done on a Xenocs Xeuss 2.0 SAXS instrument at 50 KV and 0.6 mA. The SAXS result intensity is normalized by sample thickness. Both WAXS and SAXS used Cu K_α radiation. Dynamic light scattering (DLS) tests were done on a Brookhaven BI-200SM multiangle goniometer to determine the hydrodynamic radius, R_h, of the synthesized polymers at room temperature. A 35 mW He-Ne laser with a wavelength of 632.8 nm was used. The polymers were freshly dissolved in chloroform and equilibrated for 24 h before DLS tests. The dumb-bell tensile specimens were prepared from the casted nanocomposite films by using a CEAST hollow die punch (ASTM D638 type V). Tensile tests were done at a speed of 3.0 mm/min (30 %/min) on an Instron 5569 tensile machine. 7 specimens were tested per batch to obtain the averaged tensile results. Field emission scanning electron microscope (FESEM) (JEOL JSM 6700F) was employed to observe the morphology of the specimens after tensile tests. Gold was coated on the SEM samples. UV spectra were recorded using Agilent Cary 5000 in the range of 200 nm to 800 nm at room temperature. The specimens were fabricated in the same way as the nanocomposites and the thickness is around 0.05 mm.

Results and Discussion

Synthesis and Characterization of lig-rubber-D, lig-rubber-L and lig-D

lig-rubber-D or lig-rubber-L was synthesized *via* a two-stage ring opening polymerization. First, lig-rubber was synthesized by grafting PCLLA copolymer onto lignin, which was investigated by NMR. The joint of a ε-CL block and a lactyl block shows ^{1}H NMR peaks ("a'", "b'" and "c'") and ^{13}C NMR peaks ("f'" and "g'") at different positions from either block ("a" and "g" for lactyl blocks; "b", "c" and "f" for ε-CL blocks) as shown in Fig. 1.[26, 27] From Table 1, we can see that the average length of lactyl blocks and ε-CL blocks is 1.95 and 3.23 respectively. A block length of 2.00 represents complete randomness.[27] Hence, it is seen that a quasi-random structure exists in PCLLA copolymer in which lactyl units are nearly randomly distributed while ε-CL units form short blocks. In addition, lactyl units and ε-CL units are of an equivalent amount (Table 1, CL/lactyl: 1.07), which agrees with the feeding ratio of the two monomers (L-lactide/ε-CL is 1:2, one lactide unit equals two lactyl units). In the second stage, as confirmed by ^{1}H NMR, PDLA segments were subsequently polymerized onto PCLLA to form lig-rubber-D. In Table 1 and Fig. 1a, peak "a", representing methine protons within lactyl blocks, shows substantially increased intensity in lig-rubber-D than in lig-rubber. In addition, lig-rubber-D shows decreased intensity ratio b/b' (Table 1) compared with lig-rubber. This indicates the incomplete polymerization of ε-CL in the synthesis of PCLLA copolymer and most of the remaining ε-CL monomers acted as joints in the subsequent polymerization of D-lactide. To study the importance of stereocomplex interaction in toughening commercial PLLA matrix, lig-rubber-L was synthesized in the same way as lig-rubber-D except that L-lactide was used in the second stage. Similar results can be found for lig-rubber-L from Table 1, revealing that lig-rubber-L has a similar chain structure to lig-rubber-D, which is reasonable for comparison discussed later. The molecular

masses of the synthesized polymers, calculated by ^{1}H NMR, are tabulated in Table 1.

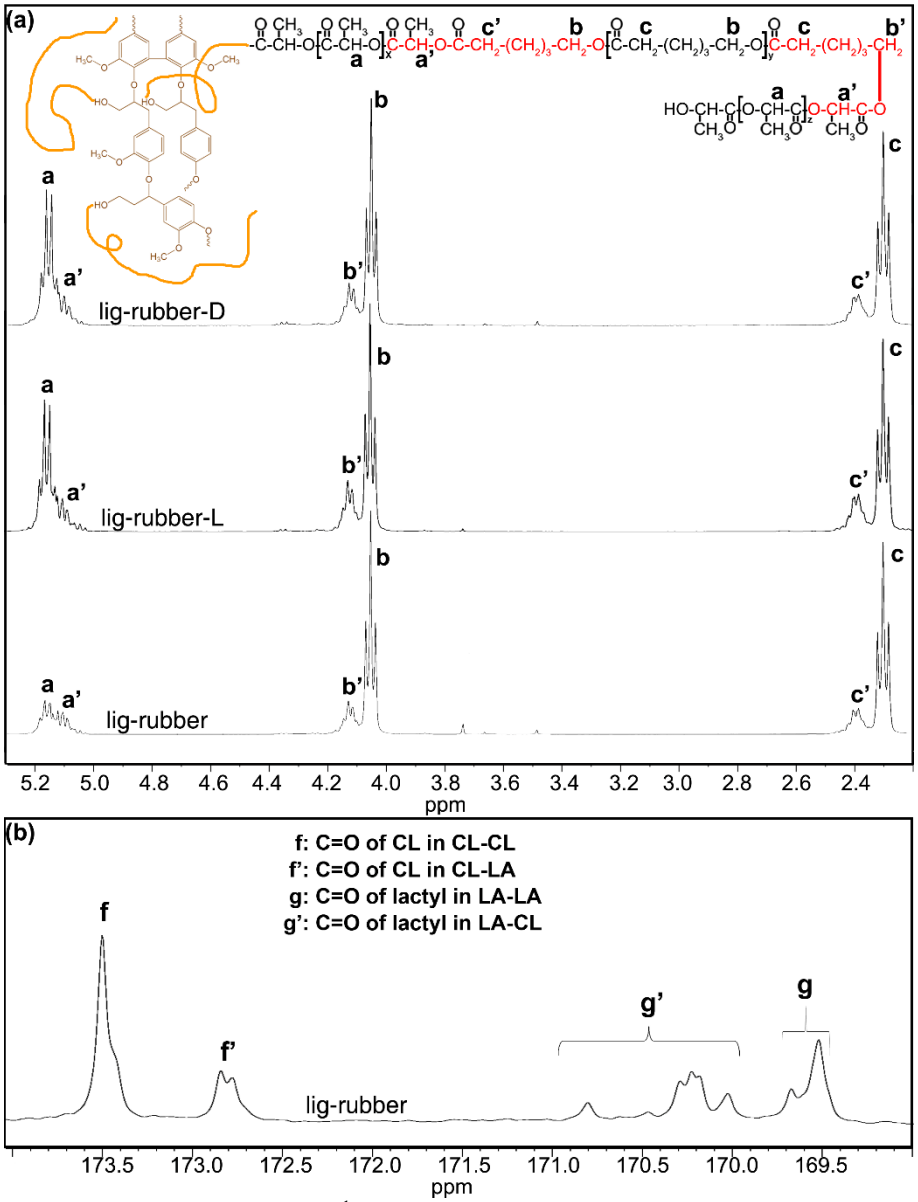

Fig. 1 NMR spectra of the synthesized polymers. (a) ^{1}H NMR spectra of lig-rubber-D, lig-rubber-L and lig-rubber; (b) ^{13}C NMR spectrum of lig-rubber (C=O signals).

Table 1 DSC and NMR data of the synthesized polymers.

Sample	DSC				NMR						
	T_g[a] (°C)	$T_{m,PCL}$ (°C)	$T_{m,sc}$ (°C)	$T_{m,\alpha}$ (°C)	M_n[b] (g/mol)	a/a'[c]	b/b'[c]	L_{CL}[d] (^{1}H)	L_{CL}[e] (^{13}C)	L_{LA}[f] (^{13}C)	CL/lactyl[g]
lig-rubber	-36	36	-	134	16065	1.5	3.71	4.71	3.23	1.95	1.07
lig-rubber-D	-17	-	158	-	20608	4.2	2.85	-	-	-	-
lig-rubber-L	-16	-	-	141	21242	3.33	2.65	-	-	-	-
lig-D	48	-	-	150	7050	-	-	-	-	-	-

[a] T_g is calculated by modulated DSC from reversing heat flow traces of the second heating run; [b] Average M_n of one polymer chain grafted on lignin estimated by ^{1}H NMR; [c] Intensity ratios of the corresponding peaks in Fig. 1a; [d] Average length of CL blocks estimated from CL signals in ^{1}H NMR spectra (b and b' in Fig. 1a) by $L_{CL}=(I_{CL\text{-}CL}/I_{CL\text{-}LA})+1$. $I_{CL\text{-}CL}$ and $I_{CL\text{-}LA}$ represents intensities of CL-CL bonds and CL-LA crossover, respectively; [e] Average length of CL blocks estimated from CL signals in ^{13}C NMR spectra (f and f' in Fig. 1b) by $L_{CL}=(I_{CL\text{-}CL}/I_{CL\text{-}LA})+1$. $I_{CL\text{-}CL}$ and $I_{CL\text{-}LA}$ represents intensities of CL-CL bonds and CL-LA crossover, respectively; [f] Average length of lactyl blocks estimated from lactyl signals in ^{13}C NMR spectra (g and g' in Fig. 1b) by $L_{LA}=(I_{LA\text{-}}$

$I_{LA/I_{LA-CL}}$)+1. I_{LA-LA} and I_{LA-CL} represents intensities of LA-LA bonds and LA-CL crossover, respectively; [g] Molar ratio calculated by using the intensities of peaks in Fig. 1b.

The synthesized polymers were further characterized by using DSC and WAXS. As shown in Table 1, when lignin was grafted with PCLLA, the resulting lig-rubber exhibits a T_g at about -36 °C which reveals the rubbery characteristic of lig-rubber at ambient conditions. On the other hand, although the rubbery PCLLA was polymerized from the mixture of the two monomers, α-form PLA homocrystallites and PCL crystallites still exist in lig-rubber, as detected by WAXS in Fig. 2. The melting points of the PLA homocrystallites and PCL crystallites in PCLLA are about 134 °C and 36 °C (Table 1) respectively, both lower than ordinary PLA and PCL melting points of 150 °C and 60 °C, respectively[37]. This demonstrates that the crystallites are imperfect in PCLLA which exhibits quasi-random nature revealed by NMR.

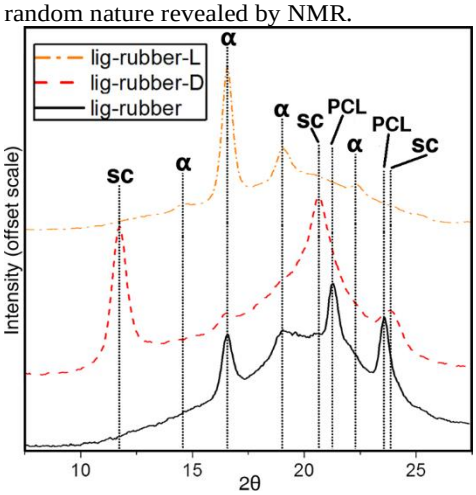

Fig. 2 WAXS diffractograms of lig-rubber-D, lig-rubber-L and lig-rubber. α stands for α-form homocrystallites,[38] and sc stands for stereocomplex crystallite.[39]

When PDLA was further grafted onto PCLLA to form lig-rubber-D, a T_g at -17 °C was detected which sits in between T_g of lig-rubber (-36 °C) and lig-D (48 °C). The outer PDLA affects the T_g of rubbery PCLLA in two aspects: First, due to the direct covalent linkage between PDLA chains and rubber-like chains, the rubber phase may exhibit reduced mobility leading to a higher T_g for rubber. Second, as shown by WAXS in Fig. 2, stereocomplex forms in lig-rubber-D, which indicates relatively strong interactions between the PCLLA L-lactyl blocks and the PDLA chains. Thus the rubber-like phase is further confined. Consequently, T_g of the rubber-like phase increases and that of PDLA decreases. On the other hand, as tabulated in Table 1, the melting point of the stereocomplex crystallites formed between L-lactyl blocks and PDLA is just 158 °C, which is well below the ordinary value of 210 °C[33]. This further demonstrates that L-lactyl block length in PCLLA is minimized and there are only imperfect stereocomplex crystallites in lig-rubber-D. For lig-rubber-L, no stereocomplex could be observed, but only homocrystallites were formed mainly from the outer PLLA (Fig. 2). The homocrystallite melting point of lig-rubber-L is 141 °C, lower than the ordinary value (150 °C), which suggests that the rubber phase may hinder the crystallization of the outer PLLA.

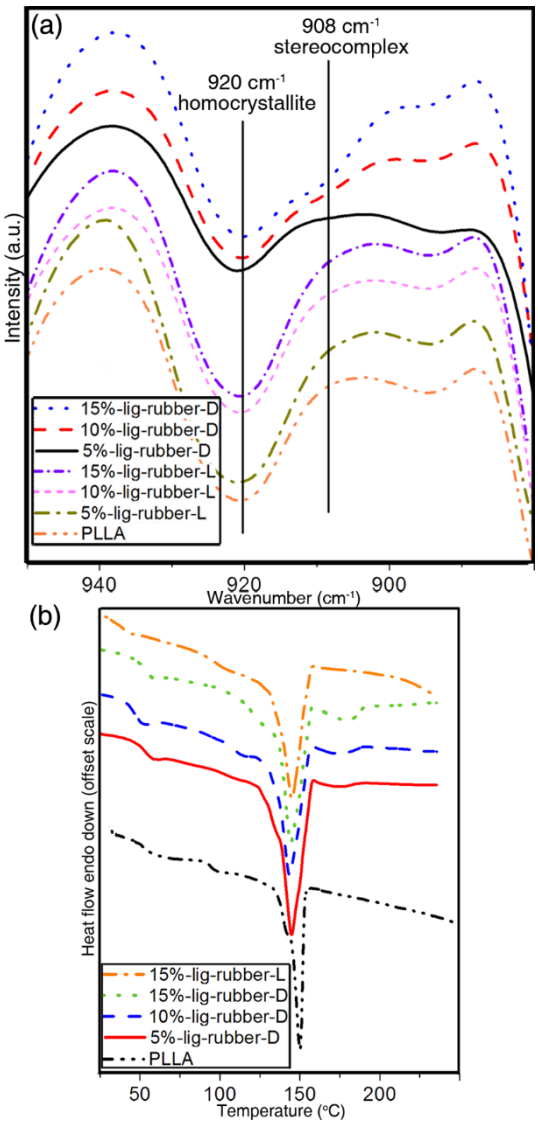

Fig. 3 FT-IR and DSC characterization of the nanocomposites. (a) FT-IR spectra from 950 cm^{-1} to 880 cm^{-1}, and (b) DSC traces of the nanocomposites.

Stereocomplexation between lig-rubber-D and PLLA Matrix

As shown in Fig. 3a, FT-IR spectra were utilized to confirm the stereocomplexation in the renewable PLA nanocomposites formed by blending commercial PLLA and lig-rubber-D. The sc-crystallites and homocrystallites of PLA exhibit different IR absorptions located at 908 cm^{-1} and 920 cm^{-1}, respectively.[30] From Fig. 3a, it can be seen that when the amount of lig-rubber-D increases, the intensity of 920 cm^{-1} absorption becomes impaired while that of the 908 cm^{-1} absorption becomes evident, confirming the occurrence of stereocomplexation between lig-rubber-D and PLLA matrix. In contrast, there is no stereocomplex absorption at 908 cm^{-1} for the PLLA/lig-rubber-L nanocomposites.

DSC was also employed to characterize the stereocomplexation between lig-rubber-D and PLLA matrix as shown in Fig. 3b. For PLLA, a single melting point exists at about 150 ℃, deriving from homocrystallites, but for the PLLA/lig-rubber-D nanocomposites, another melting point appears at about 180 ℃ deriving from sc-crystallites. With increasing lig-rubber-D contents, the sc-crystallite peak shows increased intensity while the homocrystallite peak is deteriorating, which confirms the formation of sc-crystallites between lig-rubber-D and PLLA. This stereocomplex melting point is lower than the ordinary value (~210 ℃) possibly due to two reasons: (1) PDLA segments in lig-rubber-D are too short (M_n: ~4000 g/mol, Table 1) for perfect crystallization; (2) the rubber segments in lig-rubber-D are quite long (M_n: ~16000 g/mol, Table 1) and thus could markedly confine the mobility of the outer PDLA segments during crystallization. On the other hand, for PLLA/lig-rubber-L nanocomposites, no stereocomplex could be observed.

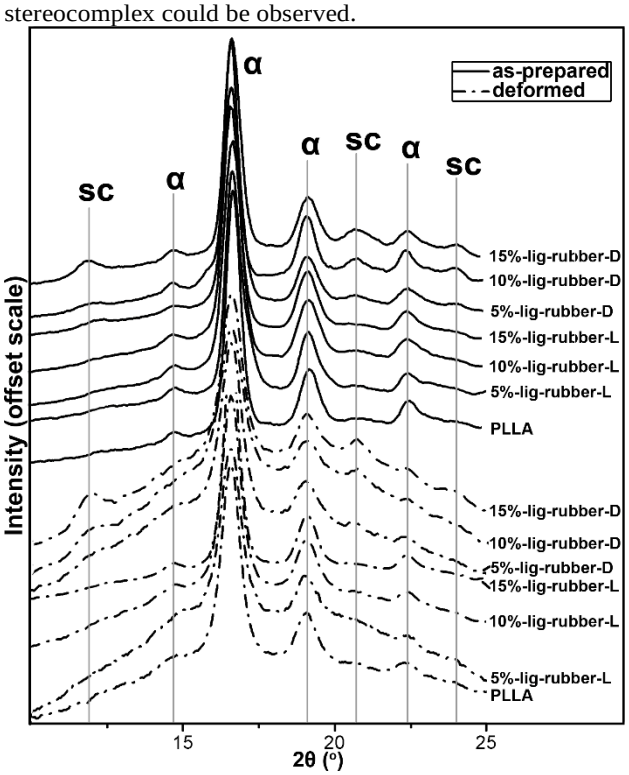

Fig. 4 WAXS diffractograms of PLLA and the nanocomposites.

Further confirmation of stereocomplexation at the interface between lig-rubber-D and matrix comes from WAXS study. As shown in Fig. 4, the WAXS diffractogram of as-prepared neat PLLA exhibits four peaks at 2θ=14.7°, 16.6°, 19.1° and 22.2°, which are characteristic of α-form homocrystallites of PLA.[38] With lig-rubber-D incorporated, the as-prepared PLLA/lig-rubber-D nanocomposites exhibit additional peaks at 2θ=11.9°, 20.7° and 23.9°, corresponding to stereocomplex crystallites of PLA,[39] which confirms the occurrence of stereocomplexation between PLLA and lig-rubber-D. In contrast, PLLA/lig-rubber-L nanocomposites show no stereocomplex peaks in WAXS diffractograms.

Effects of stereocomplex on rubber particle dispersion in PLLA matrix

The stereocomplexation between lig-rubber-D and PLLA provides a strong filler/matrix interfacial interaction and thus is supposed to facilitate lig-rubber particle dispersion in PLLA/lig-rubber-D nanocomposites, which were investigated by DLS and SAXS. The stereocomplex-facilitated dispersion is very important for mechanical properties of composites based on lig-rubber-D particles.

The hydrodynamic radius, R_h, of lig-rubber-D, lig-rubber-L, commercial PLLA and their mixtures in chloroform were measured by DLS. As can be seen in Fig. 5, although the grafted polymer on lignin helps achieve clear lig-rubber-D and lig-rubber-L solutions, both lig-rubber-D and lig-rubber-L have quite large R_h (~4 μm), indicating big aggregations in chloroform. This may be caused by the strong inter-lignin interactions including hydrogen bonding and strong π-π interactions resulting from high concentration of benzene rings in lignin. The strong inter-lignin interaction is demonstrated in Fig. 5b in which neat lignin without polymer grafted is almost completely immiscible with chloroform. When PLLA is added to form PLLA/lig-rubber-D (1:1) and PLLA/lig-rubber-L (1:1) mixtures, the aggregation is significantly reduced, which is demonstrated by much lowered R_h from the original 4000 nm to about 800 nm. R_h of PLLA/lig-rubber-D mixture is even lower, which is only 60 % of that of PLLA/lig-rubber-L mixture. The reduction of aggregation may derive from the strong interaction between the outer PLA segments of particles and the longer commercial PLLA chains. In PLLA/lig-rubber-D mixture, this interaction is even stronger and more stable due to stereocomplex formed between PDLA segments and the commercial PLLA and hence facilities better particle dispersion in comparison with PLLA/lig-rubber-L system.

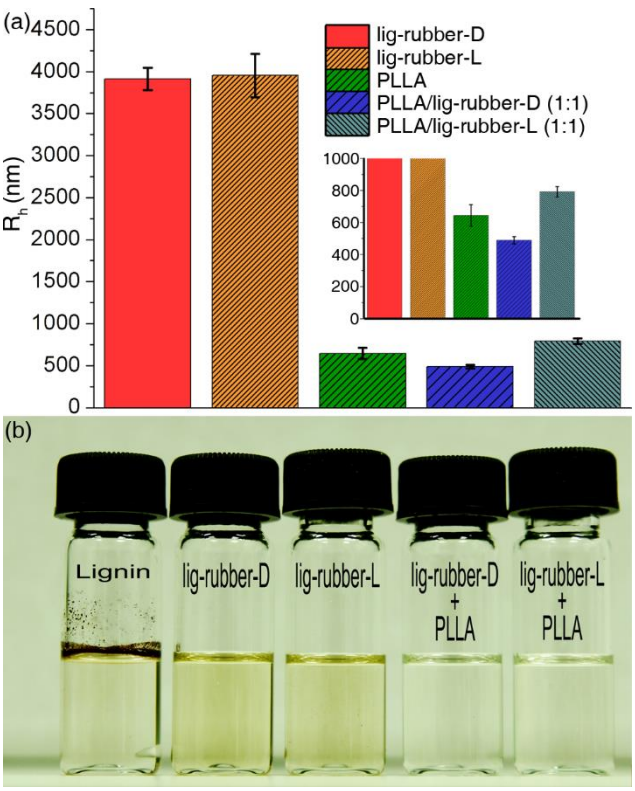

Fig. 5 (a) Hydrodynamic radius (R_h) of lig-rubber-D, lig-rubber-L, commercial PLLA and their mixtures observed in chloroform at 2 mg/ml. (b) The appearance of the chloroform solutions used in light scattering tests.

The stereocomplex-facilitated particle dispersion in PLLA/lig-rubber-D nanocomposites is also demonstrated by

SAXS, as shown in Fig. 6. For neat PLLA, there is one SAXS peak located at scattering vector q=0.034 Å^{-1}, corresponding to d-spacing of around 17.6 nm, which may derive from PLLA's lamellar structure.[40] When lig-rubber-D is mixed with PLLA, there is still only one scattering peak and the corresponding lamellar d-spacing remains almost unchanged compared with PLLA even at a high concentration of lig-rubber-D (15%-lig-rubber-D). This indicates that the stereocomplex interfacial interaction effectively facilitates lig-rubber-D dispersion in PLLA matrix. As a comparison, for PLLA/lig-rubber-L system which has no stereocomplex, SAXS shows no other significant scattering peak except the one arising from lamellar structure. However, this scattering peak shifts to a smaller q vector compared with PLLA/lig-rubber-D system, indicating a bigger lamellar d-spacing possibly caused by larger particle sizes. This again proves the effectiveness of interfacial stereocomplexation in enhancing rubber particle dispersion.

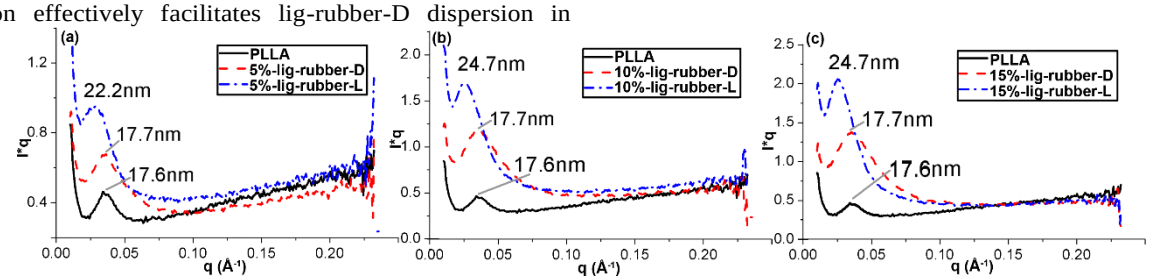

Fig. 6 SAXS diffractograms of PLLA and the nanocomposites. (a) 5 wt%, (b) 10 wt% and (c) 15 wt% of lig-rubber-D/L, where q=4πsin(θ)/λ and I*q is in counts/s.

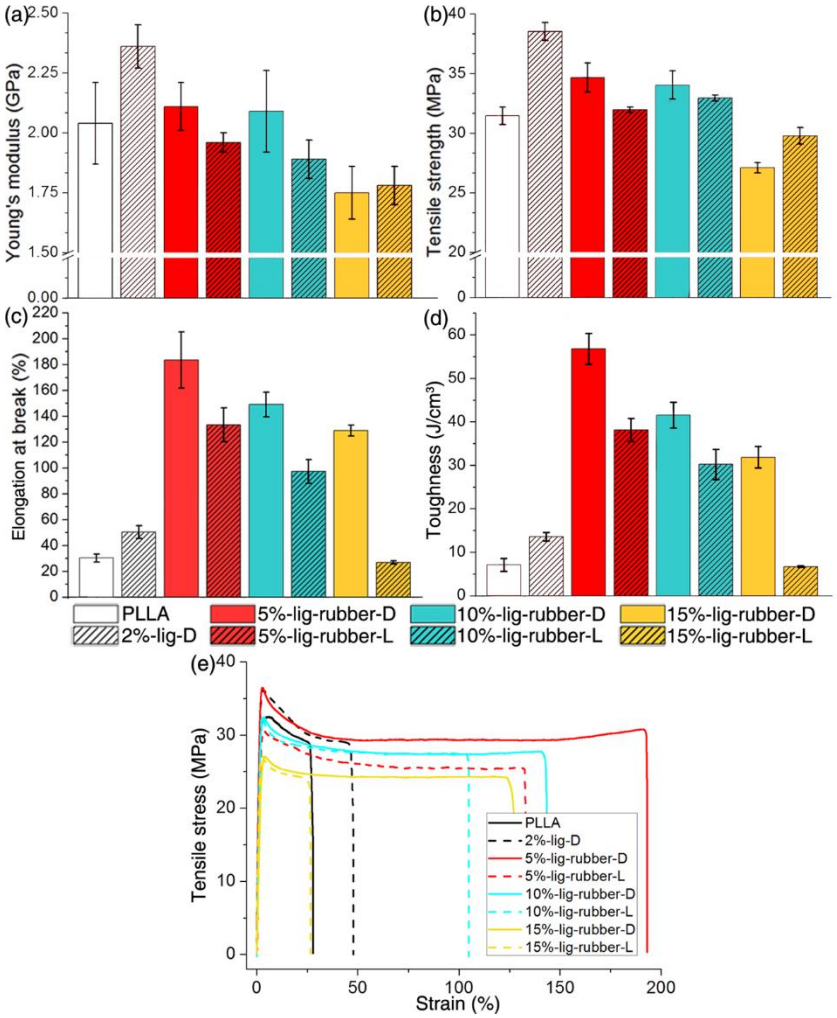

Fig. 7 Tensile mechanical properties of the renewable and biodegradable PLA nanocomposites. (a) Young's modulus. (b) Tensile strength. (c) Elongation at break. (d) Toughness, calculated by integrating the stress-strain curves of the nanocomposites. (e) Typical stress-strain curves.

Mechanical Properties

For neat commercial PLLA, the tensile strength, Young's modulus, and elongation at break are 32MPa, 2.0PGa, and 30% respectively (Fig. 7). If lig-D was introduced into PLA system, the tensile strength, Young's modulus, and elongation at break of the resulting nanocomposites containing 2 wt% of lig-D increase to 37MPa, 2.4GPa, and 45%, respectively. Similar to our previous study in which rigid POSS-PDLA filler was used in PLA system[23], both tensile strength and Young's modulus increase with the incorporation of lig-D. This could be attributed to the high mechanical property of lignin structure which consists of highly concentrated benzene rings. Furthermore, the stereocomplexation promotes load transfer from PLA to lignin, facilitates lignin dispersion in PLLA and thus is considered to result in the enhanced tensile strength and modulus of PLLA/lig-D composites. However, different from our previous study in POSS-PDLA system which shows a significant reduction of elongation at break[23], the elongation at break in the PLLA/lig-D system increases by 50% compared with neat PLLA. This may result from the flexibility of lignin structure in which benzenes are linked with ether linkages, while POSS is a very rigid inorganic structure.

When a rubbery layer was inserted into lig-D to form lig-rubber-D, the toughening effect was substantially enhanced while other mechanical properties such as tensile strength and Young's modulus were maintained. As shown in Fig. 7, with the incorporation of 5 wt% of lig-rubber-D into PLLA, the resulting nanocomposites (5%-lig-rubber-D) exhibit a seven-fold enhancement in toughness (calculated by integrating the stress-strain curves) compared with neat PLLA, which is sizable considering that 5%-lig-rubber-D contains only 3.8 wt% of rubber. Simultaneously, the tensile strength and Young's modulus of 5%-lig-rubber-D also increase by 10% and 5% respectively.

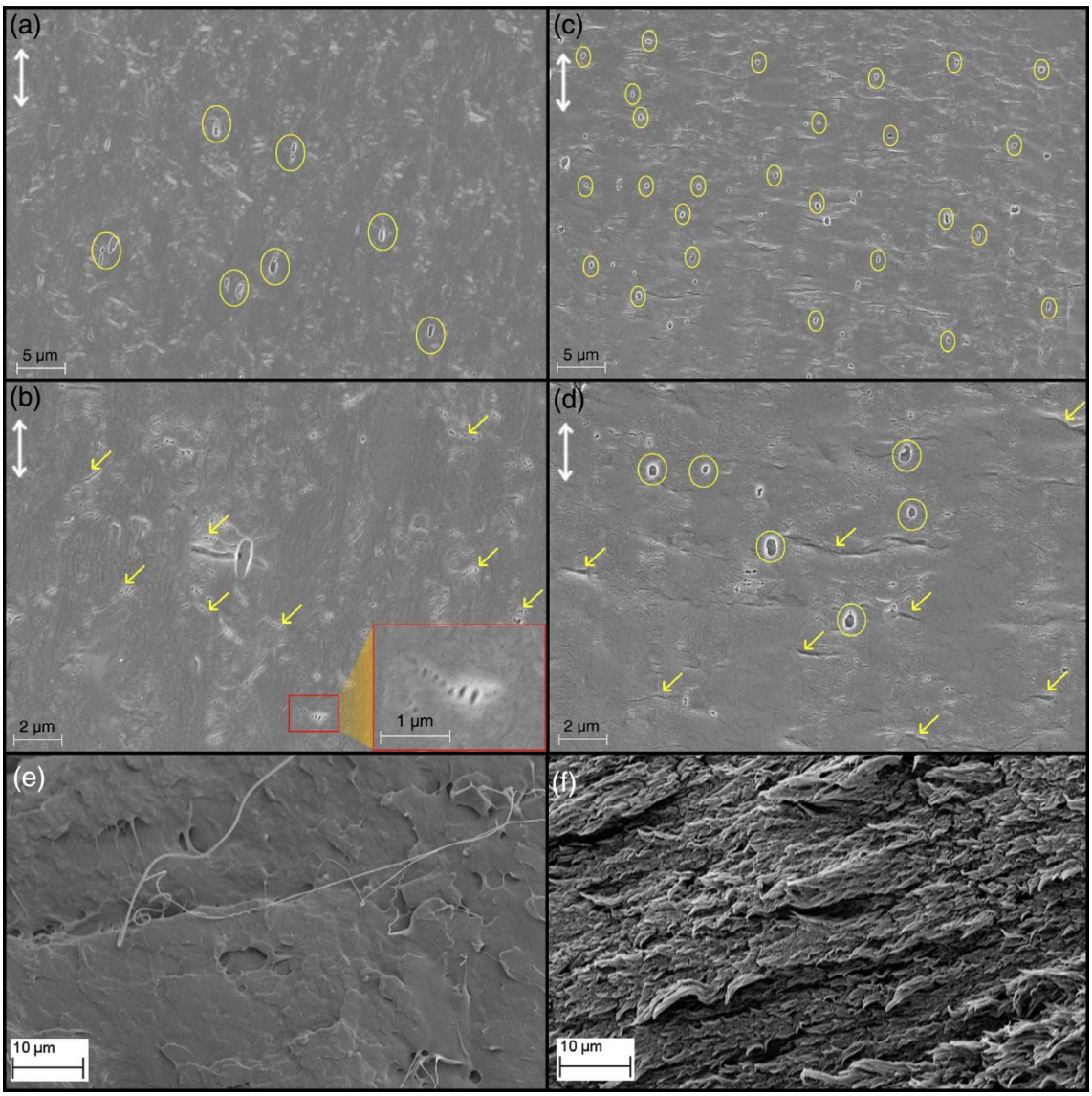

Fig. 8 (a-d) SEM images of the film surface near the fracture tip after tensile tests, in which the double-head arrows point the tensile direction. (a-b) 15%-lig-rubber-D, (c-d) 15%-lig-rubber-L. The inset of (b) is the enlargement of the area in the rectangle. (e-f) The cross-sectional fracture surface of (e) neat PLLA and (f) 15%-lig-rubber-D.

The mechanism of the significant enhancement in mechanical properties is illuminated by SEM study. The morphology of the sample film surface after tensile tests is shown in Fig. 8a-d. In PLLA/lig-rubber-D nanocomposites, the rubber layers at lignin/PLLA interface may initiate crazes and crazing is considered as the key toughening mechanism.[41] In response to deformation, craze nuclei initiated by rubber layers would develop into mature crazes, as pointed by arrows in Fig. 8b, to absorbe energy. Consequently, the PLLA/lig-rubber-D nanocomposites exhibit remarkable improvements in toughness compared with neat PLLA and PLLA/lig-rubber-D has a much rougher fracture surface than PLLA (Fig. 8e-f). As a comparison, lignin grafted with PDLA without rubber layers, i.e., lig-D, was added to form PLLA/lig-D nanocomposites. From Fig. 7, we can see that the resulting 2%-lig-D shows only a slight increase in toughness compared with PLLA, although 2%-lig-D possesses similar amounts of lignin to 5%-lig-rubber-D. This also confirms the toughening effect of rubber layers in lig-rubber-D.

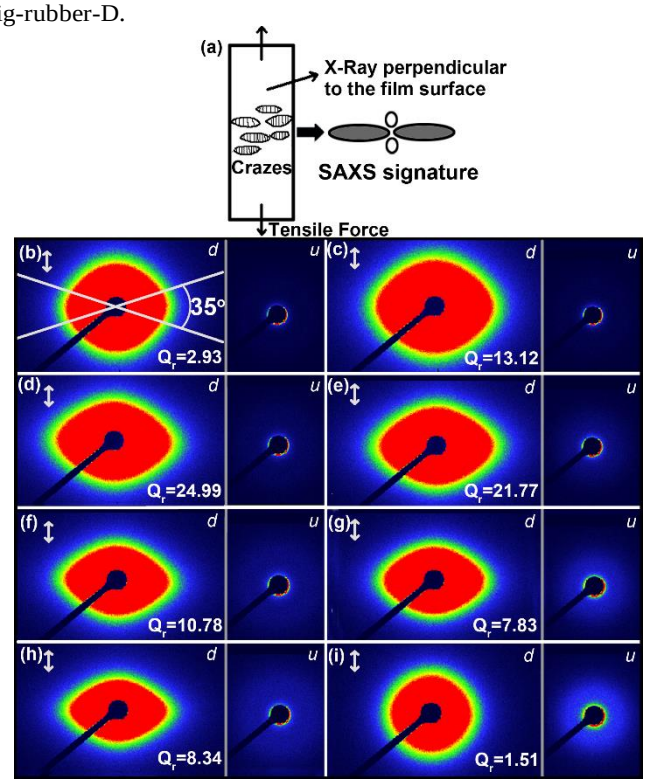

Fig. 9 (a) The direction of tensile force/incident X-ray and the expected SAXS signature from crazes. (b-i) SAXS scattering patterns of (b) PLLA, (c) 2%-lig-D, (d) 5%-lig-rubber-D, (e) 5%-lig-rubber-L, (f) 10%-lig-rubber-D, (g) 10%-lig-rubber-L, (h) 15%-lig-rubber-D and (i) 15%-lig-rubber-L. Double-head arrows indicate the tensile direction. *d* and *u* stand for *deformed* and *undeformed*, respectively. Q_r is the relative invariant related with craze concentration.

To further characterize craze formation initiated by rubber phase at lignin/PLLA interface, SAXS was utilized. As shown in Fig. 9a, fibrils inside crazes would scatter X-ray to form the equatorial strip of the SAXS signature, which has a quantitative relation with craze concentration.[42, 43] Hence, we made use of the 35° equatorial sector area of the SAXS pattern (Fig. 9b) to obtain quantatitive information on craze concentration through invariant analysis as follows:

$$Q_r = \int_{q_1}^{q_2} I(q)qdq + Q_{tail} \qquad (1)$$

$$Q_{tail} = \int_{q_2}^{\infty} I(q)qdq \qquad (2)$$

where Q_r is a relative invariant, q is the scattering vector and $I(q)$ is the scattering intensity from crazes. Craze concentration can be probed by Q_r.

In Fig. 9b-d, PLLA, 2%-lig-D and 5%-lig-rubber-D all exhibit elliptical SAXS patterns after deformation, which indicates the formation of crazes. By integrating the equatorial sector areas of the elliptical SAXS patterns according to Equation (1) and (2), the relative invariants of PLLA, 2%-lig-D and 5%-lig-rubber-D are calculated to be 2.93, 13.12 and 24.99, respectively. This demonstrates that the flexible structure of lignin facilitates craze formation and moreover the insertion of rubber phase into lignin/PLLA interface is especially effective in initiating crazes resulting in a substantially higher craze concentration.

However, with a further increase of lig-rubber-D concentration, the tensile strength and Young's modulus were gradually impaired (Fig. 7), mainly due to high rubber content. An interseting obvervation is that with an increase of lig-rubber-D content, for example in 10%-lig-rubber-D and 15%-lig-rubber-D systems, elongation at break is also reduced compared with that of 5%-lig-rubber-D system, although they still have much higher elongation at break than neat PLA and the PLLA/lig-D system. The possible mechanism is that at high concentrations of lig-rubber-D, the inter-lignin particle distance is reduced. With so many lig-rubber-D particles and much shorter distances between them, rubber-phase-induced crazes will develop into cracks before they are fully developed and lead to premature failure of polymer composites, which can be confirmed by SAXS as shown in Fig. 9. The relative invariant, Q_r, is 24.99, 10.78 and 8.34 for 5%-lig-rubber-D (Fig. 9d), 10%-lig-rubber-D (Fig. 9f) and 15%-lig-rubber-D (Fig. 9h), respectively, revealing that craze concentration is reduced in the fractured sample with more lig-rubber-D incorporated.

In addition, filler/matrix interfacial interaction is another important factor in determining the morphology and mechanical property of polymer composites. As shown by light scattering experiments (Fig. 5) and SAXS (Fig. 6), the stereocomplex interaction between PDLA of lig-rubber-D and commercial PLLA facilitates better dispersion of lig-rubber-D particles in the nanocomposite system compared with the PLLA/lig-rubber-L system. Besides, the stereocomplex interaction also enhances load transfer between the matrix and fillers, which is quite stable during deformation as demonstrated by WAXS in Fig. 4. The WAXS diffractograms of deformed PLLA/lig-rubber-D nanocomposites still obviously exhibit peaks characteristic of stereocomplex-crystallites. The influence of strong stereocomplex interaction could also be illustrated by SEM in Fig. 8. For PLLA/lig-rubber-D nanocomposites (Fig. 8a-b), the stereocomplex-facilitated desirable particle dispersion results in a homogeneous craze distribution, in which most crazes could fully develop into mature ones and absorb more energy; while for PLLA/lig-rubber-L (Fig. 8c-d), rubber particles are aggregated in a less homogeneous distribution, which leads to more cavitation/voids (labelled by circles in Fig. 8) and "giant" crazes (labelled by arrows in Fig. 8d). In the case of PLLA/lig-rubber-L, due to

aggregation, rubber particles conversely act as the source of polymer breakdown and hence the toughening effect is reduced. Consistent results are obtained by SAXS as shown in Fig. 9. The relative invariant of PLLA/lig-rubber-L system is much smaller than that of PLLA/lig-rubber-D system, indicating substantially lower craze concentrations due to rubber aggregation in PLLA/lig-rubber-L nanocomposites. As a result (Fig. 7), PLLA/lig-rubber-D nanocomposites have substantially improved toughness; while PLLA/lig-rubber-L, which contains no stereocomplex, exhibits improvement in toughness to a much smaller extent. Particularly, 15%-lig-rubber-L shows even lower toughness than neat PLA.

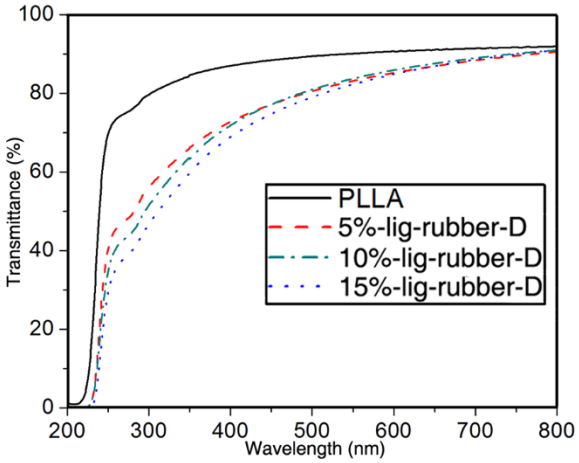

Fig. 10 UV spectra of PLLA and the PLLA/lig-rubber-D nanocomposites.

UV Barrier Property

UV light barrier property is important for packaging materials in terms of protecting light-sensitive products during storage. PLA is widely used as a packaging material, but its poor UV barrier property limits its application.[44] The UV barrier property of PLLA and the PLLA/lig-rubber-D nanocomposites is demonstrated in Fig. 10. With the incorporation of lig-rubber-D into PLLA, the resulting nanocomposites exhibit much better UV light barrier property, which blocks about half of UV-C (100-280 nm) and UV-B (280-315 nm) and about 30% of UV-A (315−400 nm). With less than 0.15 wt% of lignin in the nanocomposites, the good UV barrier property is mainly attributed to the homogeneous dispersion of lig-rubber-D particles.

Conclusions

A series of renewable and fully biodegradable PLA-based nanocomposites were successfully fabricated by blending lignin-rubber-PDLA (lig-rubber-D) and commercial PLLA in chloroform. In the synthesis of lig-rubber-D, poly (ε-caprolactone-*co*-lactide) (PCLLA) rubbery layer was grafted on lignin *via* ring opening copolymerization of ε-caprolactone/L-lactide mixture, followed by the formation of poly (D-lactide) (PDLA) outer segments *via* polymerization of D-lactide. NMR revealed a quasi-random structure of PCLLA and verified the subsequent formation of PDLA segments. MDSC confirmed the rubbery characteristic of PCLLA copolymer at ambient conditions. FTIR, DSC and WAXS demonstrated that stereocomplexation occurs between lig-rubber-D and PLLA, which acts as the strong matrix/filler interfacial interaction. Furthermore, light scattering and SAXS studies showed that dispersion of lig-rubber-D could be facilitated by stereocomplex interactions between lig-rubber-D and PLLA matrix. The resulting PLLA/lig-rubber-D systems exhibited up to seven-fold increase in toughness and simultaneous improvement in modulus and tensile strength. Crazing is considered as the important toughening mechanism. Besides, the stereocomplex between matrix and lig-rubber-D and the rubber phase which mediates at the interface of matrix and lignin are the potential origins of simultaneously enhanced toughness and strength of the nanocomposites. The toughened PLA nanocomposites also had desirable UV light barrier property, which together with the excellent mechanical performances endows the nanocomposites with good potential in packaging applications.

Acknowledgements

The authors acknowledge the financial support (R-284-000-084-133) to the present research and scholarship to Sun Yang provided by National University of Singapore. The authors are also grateful for the use of equipment in materials analysis in Institute of Materials Research and Engineering (IMRE), under the Agency of Science, Technology, and Research (A*STAR). The authors appreciate Mr. Tang Tao and Dr. Yuan Du in UV absorption and SEM experiments.

Notes and references

[a] Department of Materials Science & Engineering, National University of Singapore, 9 Engineering Drive 1, Singapore 117576. Email: msehc@nus.edu.sg

[b] Institute of Chemical and Engineering Science, Agency for Science, Technology and Research (A*STAR), 1 Pesek Road, Jurong Island, Singapore 627833

[c] School of Materials Science and Engineering, Nanyang Technological University, Block N4.1, Nanyang Avenue, Singapore 639798

[d] Institute of Materials Research and Engineering, Agency for Science, Technology and Research (A*STAR), 3 Research Link, Singapore 117602. Email: cb-he@imre.a-star.edu.sg

1. W. O. Doherty, P. Mousavioun and C. M. Fellows, *Industrial Crops and products*, 2011, **33**, 259-276.
2. K. V. Sarkanen and C. H. Ludwig, *Lignins: occurrence, formation, structure and reactions.*, 1971.
3. J. M. Cruz, J. M. Dom ńguez, H. Dom ńguez and J. C. Paraj ó, *Journal of agricultural and food chemistry*, 2001, **49**, 2459-2464.
4. V. Ugartondo, M. Mitjans and M. P. Vinardell, *Bioresource technology*, 2008, **99**, 6683-6687.
5. K. Toh, S. Nakano, H. Yokoyama, K. Ebe, K. Gotoh and H. Noda, *Polymer Journal*, 2005, **37**, 633-635.
6. S. Kumar, A. Mohanty, L. Erickson and M. Misra, *Journal of Biobased Materials and Bioenergy*, 2009, **3**, 1-24.
7. Y. S. Kim and J. F. Kadla, *Biomacromolecules*, 2010, **11**, 981-988.

8. T. Nemoto, G. i. Konishi, Y. Tojo, Y. C. An and M. Funaoka, *Journal of Applied Polymer Science*, 2012, **123**, 2636-2642.
9. G. Sena-Martins, E. Almeida-Vara and J. Duarte, *Industrial Crops and products*, 2008, **27**, 189-195.
10. W. de Oliveira and W. G. Glasser, *Macromolecules*, 1994, **27**, 5-11.
11. T. Lindström, *Colloid & Polymer Science*, 1979, **257**, 277-285.
12. Y. Deng, X. Feng, D. Yang, C. Yi and X. Qiu, *BioResources*, 2012, **7**.
13. R. E. Drumright, P. R. Gruber and D. E. Henton, *Advanced Materials*, 2000, **12**, 1841-1846.
14. H. Tsuji, S. Yamamoto and A. Okumura, *Journal of Applied Polymer Science*, 2011, **122**, 321-333.
15. R. Bhardwaj and A. K. Mohanty, *Biomacromolecules*, 2007, **8**, 2476-2484.
16. W. Ouyang, Y. Huang, H. Luo and D. Wang, *Journal of Polymers and the Environment*, 2012, **20**, 1-9.
17. J. Li, Y. He and Y. Inoue, *Polymer international*, 2003, **52**, 949-955.
18. Y.-L. Chung, J. V. Olsson, R. J. Li, C. W. Frank, R. M. Waymouth, S. L. Billington and E. S. Sattely, *ACS Sustainable Chemistry & Engineering*, 2013, **1**, 1231-1238.
19. S. M. Ye, T. T. Lin, W. W. Tjiu, P. K. Wong and C. B. He, *Journal of Applied Polymer Science*, 2013, **128**, 2541-2547.
20. A. Bhatia, R. K. Gupta, S. N. Bhaftacharya and H. J. Choi, *Korea-Australia Rheology Journal*, 2007, **19**, 125-131.
21. H. Z. Liu, F. Chen, B. Liu, G. Estep and J. W. Zhang, *Macromolecules*, 2010, **43**, 6058-6066.
22. T. N. Li, L. S. Turng, S. Q. Gong and K. Erlacher, *Polymer Engineering and Science*, 2006, **46**, 1419-1427.
23. Y. Sun and C. He, *Macromolecules*, 2013, **46**, 9625-9633.
24. H. T. Qian, J. Z. Bei and S. G. Wang, *Polymer Degradation and Stability*, 2000, **68**, 423-429.
25. P. Purnama, Y. Jung and S. H. Kim, *Macromolecules*, 2012, **45**, 4012-4014.
26. H. R. Kricheldorf, K. Ahrensdorf and S. Rost, *Macromolecular Chemistry and Physics*, 2004, **205**, 1602-1610.
27. H. R. Kricheldorf, K. Bornhorst and H. Hachmann-Thiessen, *Macromolecules*, 2005, **38**, 5017-5024.
28. J. Xie, M. Ihara, Y. M. Jung, I. K. Kwon, S. H. Kim, Y. H. Kim and T. Matsuda, *Tissue Engineering*, 2006, **12**, 449-458.
29. H. Tsuji, *Macromolecular Bioscience*, 2005, **5**, 569-597.
30. E. M. Woo and L. Chang, *Polymer*, 2011, **52**, 6080-6089.
31. J. Narita, M. Katagiri and H. Tsuji, *Macromolecular Materials and Engineering*, 2011, **296**, 887-893.
32. H. Xu, S. Tang, J. Chen, P. Yin, W. Pu and Y. Lu, *Polymer Bulletin*, 2011, 1-17.
33. Y. Sun and C. B. He, *Acs Macro Letters*, 2012, **1**, 709-713.
34. Y. Sun and C. B. He, *Rsc Advances*, 2013, **3**, 2219-2226.
35. S. Brochu, R. E. Prud'Homme, I. Barakat and R. Jerome, *Macromolecules*, 1995, **28**, 5230-5239.
36. T. T. Lin, X. Y. Liu and C. He, *Polymer*, 2010, **51**, 2779-2785.
37. R. Renstad, S. Karlsson, Å. Sandgren and A.-C. Albertsson, *Journal of environmental polymer degradation*, 1998, **6**, 209-221.
38. J. Zhang, K. Tashiro, H. Tsuji and A. J. Domb, *Macromolecules*, 2007, **40**, 1049-1054.
39. J. Zhang, H. Sato, H. Tsuji, I. Noda and Y. Ozaki, *Journal of Molecular Structure*, 2005, **735-736**, 249-257.
40. J. Cho, S. Baratian, J. Kim, F. Yeh, B. S. Hsiao and J. Runt, *Polymer*, 2003, **44**, 711-717.
41. C. He, A. M. Donald and M. F. Butler, *Macromolecules*, 1998, **31**, 158-164.
42. C. He, A. M. Donald, M. F. Butler and O. Diat, *Polymer*, 1998, **39**, 659-667.
43. C. He, T. Liu, W. C. Tjiu, H.-J. Sue and A. F. Yee, *Macromolecules*, 2008, **41**, 193-202.
44. R. Auras, B. Harte and S. Selke, *Macromolecular Bioscience*, 2004, **4**, 835-864.